

Negative dimensions of the turbulent dissipation field

Jaap Molenaar

Mathematics Department, Eindhoven University of Technology, P.O. Box 513, 5600 MB Eindhoven, The Netherlands

Janine Herweijer and Willem van de Water

Physics Department, Eindhoven University of Technology, P.O. Box 513, 5600 MB Eindhoven, The Netherlands

(Received 24 October 1994)

Random multifractals that involve ensemble-averaged partition sums may give rise to negative dimensions. These models are highly relevant for interpreting fluctuations in fully developed hydrodynamic turbulence. From the experimental results that are obtained in a laboratory turbulent flow, it appears that self-similarity of the partition sums is only reached asymptotically. We demonstrate that this effect is due to correlations between subsequent refinements in a multifractal description. We give a way of correcting for the effects of correlations. We analyze an exactly solvable model that has the correlation depth as a parameter. This model has asymptotic self-similarity and displays a phase transition behavior in the limit of infinite deterministic refinements.

PACS number(s): 47.27.-i, 02.50.-r, 05.45.+b, 47.53.+n

I. INTRODUCTION

It is now widely believed that the spatial organization of turbulent dissipation has multifractal properties [1]. It implies that the dissipation $\epsilon(l)$ inside a volume element of linear size l has local scaling behavior with a scaling exponent α , $\epsilon(l) \simeq l^\alpha$. There is a whole range of α values, each of these being distributed in its own fractal set with fractal dimension $f(\alpha)$. A long stretch of dissipation on a line that cuts through a turbulent dissipation field is then thought to contain many realizations of a fractal process. Naively, each of those realizations would suffice to compute a complete spectrum $f(\alpha)$ of scaling exponents. The data requirements for determining $f(\alpha)$ in an experiment therefore seem to be quite modest. This is quite surprising in view of the extreme data requirements for measuring the scaling of turbulent structure functions. The structure function $G_p(r)$ is defined as $G_p(r) = \langle [\Delta u(r)]^p \rangle_x$, where $\Delta u(r) = u(x+r) - u(x)$ is a velocity difference over a distance r . The structure function has scaling behavior $G_p(r) \simeq r^{\zeta(p)}$. A dependable estimate of $\zeta(p)$ for $p \approx 10$ needs millions of integral length scales [2].

Although determination of the exponents α of the dissipation field may be done from a few integral length scales, the resulting $f(\alpha)$ was shown to fluctuate wildly from sample to sample [3]. It was realized that averaging the $f(\alpha)$ determined from intervals stretching a few integral length scales was not a proper way of analyzing these fluctuations [4]. The crucial point is the order of performing averages and taking logarithms.

In order to appreciate this, let us recall that the spectrum $f(\alpha)$ of scaling exponents is determined through the partition sum

$$\Gamma(q, \tau) = \frac{1}{l^{\tau(q)}} \sum_i \epsilon_i^q(l), \quad (1)$$

where the sum is over the dissipation integrated over elements i of a covering of linear size l . In the limit of vanishing l (infinite refinement) the condition $\Gamma = 1$ singles out a function $\tau(q)$ that is related to $f(\alpha)$ through a Legendre transformation. The key point is that the *partition sum* should be averaged over many different realizations of the fractal process and *not* the function $\tau(q)$. The ensemble average of the partition sum then defines a function $\tau(q)$ through

$$\left\langle \sum_i \epsilon_i^q(l) \right\rangle \simeq l^{\tau(q)}, \quad (2)$$

where the angular brackets denote the ensemble average. The definition has the consequence that $f(\alpha)$ can become *negative*. Negative dimensions are associated with α values that occur less than once in a typical ensemble member. As pointed out in Ref. [5], direct ways to determine $f(\alpha)$ through the processing of histograms of local scaling exponents will have trouble when $f(\alpha) < 0$ because the chances of encountering the corresponding scaling exponents actually *decrease* when decreasing the scale l . A quite interesting solution to this problem was suggested by Chhabra and Sreenivasan [5], who proposed to evaluate the averaged partition sum in Eq. (2) at a fixed scale using the method of multipliers.

In order to understand this method we realize that in the standard experimental setup, the turbulence dissipation is measured on a line. Imagine that a linear interval of length l_1 is cut into a pieces of length $l_2 = l_1/a$. The question then is about the ratio of the integrated dissipation on the daughter interval l_2 to that of the mother interval l_1 , $m_{i,j} = \epsilon_{i,j}(l_2)/\epsilon_j(l_1)$, where the index $i = 1, \dots, a$ points to a particular daughter interval of l_2 and the index j points to a given mother interval. The multipliers are the numbers $m_{i,j}$ of such a partition. The following argument demonstrates that multipliers have scaling properties if the multiplier $m_{i,j}$ is not

correlated with the dissipation $\epsilon_j(l_1)$.

To this aim the ensemble-averaged partition sum Eq. (2) is written as

$$\begin{aligned} l_2^{\tau(q)} &\simeq \left\langle \sum_{i,j} \epsilon_{i,j}^q(l_2) \right\rangle \\ &= \sum_{i,j} \langle m_{i,j}^q \epsilon_j^q(l_1) \rangle \\ &= \sum_i \langle m_i^q \rangle \sum_j \langle \epsilon_j^q(l_1) \rangle \simeq \sum_i \langle m_i^q \rangle l_1^{\tau(q)}, \end{aligned} \quad (3)$$

where we have used the absence of correlation between multiplier $m_{i,j}$ and mother dissipation ϵ_j to factorize the average product into the product of averages. Therefore,

$$\left\langle \sum_{i=1}^a m_i^q \right\rangle = a^{-\tau(q)}. \quad (4)$$

The partition sum in Eq. (4) is at a fixed scale, but the derivation of Eq. (4) has assumed the scaling behavior of the full partition sum [Eq. (2)]. According to Eq. (3), the scaling function $\tau(q)$ can be computed at any number of partitions a and does not depend on a (a is called the *base* of the multiplier distribution). The use of multipliers to analyze self-similar facets of turbulence has received considerable attention in the turbulence literature [6]. In particular we would like to point to the pioneering work of Novikov [7].

It was found in experiments that even in high Reynolds number turbulence the function $\tau(q)$ still has a weak dependence on the base a [3]

$$\tau_a(q) = \tau(q) + \frac{K(q)}{\log a}. \quad (5)$$

Therefore, the fractal set that is associated with turbulent dissipation displays only *asymptotic* scale invariance.

Figure 1 shows the result for the scaling function $f(\alpha)$ in a turbulent air flow (the experiment is detailed in Sec. IV). The function $f(\alpha)$ was determined from measured functions $\tau(q)$ at values of the multiplier base a , $a = 2, \dots, 9$. The scaling functions that were directly derived from the experiment are shown in Fig. 1(a). They have been corrected in Fig. 1(b) using a correction function $K(q)$ as in Eq. (5). The corrected scaling functions show a significantly smaller variation with a than the raw results in Fig. 1(a), thus demonstrating the relevance of Eq. (5) for experiments.

Because of its importance for analyzing turbulence experiments, it is necessary to have a complete understanding of the emergence of correction functions as in Eq. (5). This is the prime goal of this paper. We will argue that asymptotic self-similarity [such as that in Eq. (5)] is a direct consequence of nonzero correlations between multipliers at different refinement levels. In Sec. II we will discuss analytically solvable generalizations of random Cantor sets that display correlations between subsequent refinement levels. The strength of these correlations depends on a parameter in the model. At one extreme value of this parameter, the correlation is complete and refinement is deterministic after it has been

seeded randomly. At the other extreme, subsequent refinements are completely independent. We will show that in the limit of infinite refinements a *phase transition phenomenon* arises when correlations are complete. Section II highlights the key results of our analysis. Mathematical detail is diverted to the Appendixes.

It turns out that there is a simple relation between the function $K(q)$ and the extent of the correlations. In Sec. III we discuss the way in which the scaling function $\tau(q)$ is derived from measured distributions of multipliers. Finally, in Sec. IV the results of an experiment in laboratory turbulence are given. We conclude with a discussion of the results in Sec. V.

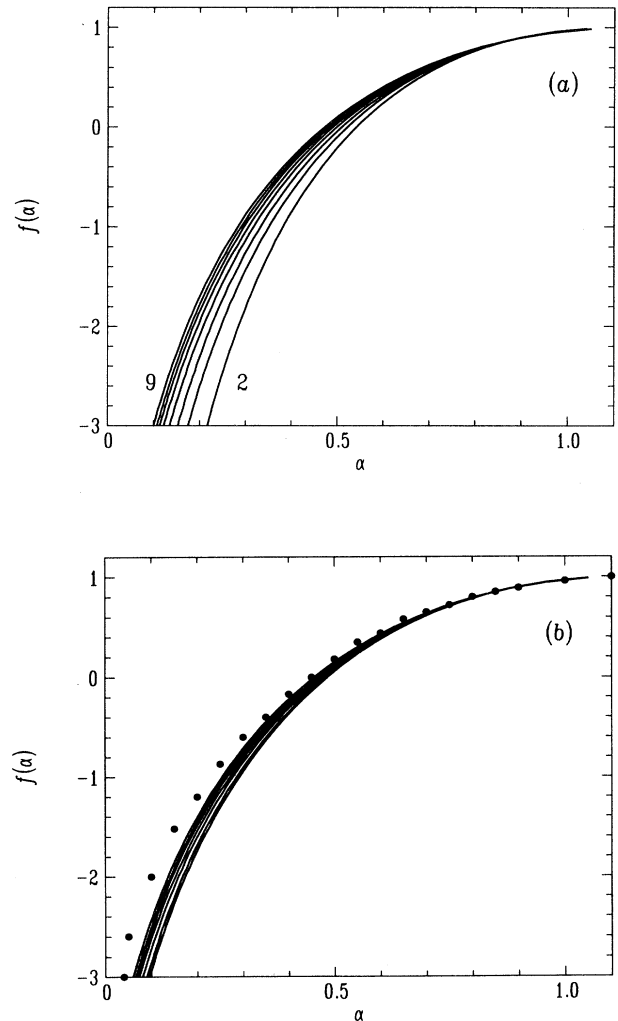


FIG. 1. Measured multiplier scaling functions of turbulent dissipation $f(\alpha)$ at scale $r/\eta = 570$ for bases ranging from $a = 2$ to $a = 9$. The dissipation was measured in a turbulent jet at a Reynolds number $R_\lambda = 8 \times 10^2$. (a) Without taking into account the asymptotic correction function $K(q)$. (b) Lines, with correction function $K(q)$ computed from $a = 2, 4$; dots, results from Chhabra and Sreenivasan [3] that were obtained in atmospheric turbulence.

II. RANDOM FRACTALS WITH FIXED SCALES

Let us consider fractals that randomly redistribute the measure when the scale is reduced. In our model we generate subintervals upon descending the cascade by successively halving the original interval. So at level i the fractal consists of 2^i intervals of length 2^{-i} , which together still cover the unit interval. While each interval at level $i-1$ is split up into two half, the left half inherits a fraction x_i and the right half a fraction $1-x_i$ of the total measure of the original interval. To proceed to refinement level n , we need n stochastic variables $x_i, i = 1, \dots, n$, which are drawn from a simultaneous probability distribution $P(x_1, \dots, x_n)$. We emphasize the usage of the joint probability distribution function as we will concentrate on *correlations* between successive x_i and x_{i+1} . We will always impose the nonessential condition that x_1 be distributed uniformly.

The partition function of the random fractal built up this way is given by

$$\Gamma_n(q, \tau) = 2^{n\tau} \sum_{j=1}^{2^n} p_{n,j}^q, \quad (6)$$

with $p_{n,j}$ the measure of the j th interval at level n . It has the form

$$p_{n,j} = r_1 r_2 \cdots r_n \quad (7)$$

with $r_i = x_i$ or $1-x_i, i = 1, \dots, n$. The sequence of x_i and $1-x_i$ in the product Eq. (7) is as the sequence of 0 and 1 in a binary expansion of the index j . The scaling function $\tau_n(q)$ at level n follows from the condition

$$\langle \Gamma_n(q, \tau_n) \rangle = 1 \quad (8)$$

or

$$\tau_n(q) = -1 - \frac{1}{n} \log_2 \left(\sum_{j=1}^{2^n} \langle p_{n,j}^q \rangle \right). \quad (9)$$

The averages $\langle p_{n,j}^q \rangle$ are to be determined from the joint probability distribution $P(x_1, \dots, x_n)$. By a conspicuous choice of this distribution we can adjust the degree of correlation between subsequent x_i and x_{i+1} . We will use the standard correlation function to gauge the correlation strength

$$C(i, i') = \frac{\langle x_i x_{i'} \rangle - \langle x_i \rangle \langle x_{i'} \rangle}{[(\langle x_i^2 \rangle - \langle x_i \rangle^2)(\langle x_{i'}^2 \rangle - \langle x_{i'} \rangle^2)]^{1/2}}. \quad (10)$$

For the models that we consider, the correlation function behaves as

$$C(i, i') \sim \exp(-|i - i'|/\xi), \quad (11)$$

where we call ξ the correlation depth. In the following subsections we consider three cases: complete independence of x_i and x_{i+1} , zero correlation depth ($\xi = 0$) (Sec. II A); complete correlation, infinite correlation depth ($\xi = \infty$) (Sec. II C); and intermediate correlation

depth ($0 < \xi < \infty$) (Sec. II D).

A random redistribution of the *measure* is but one way of constructing Cantor-like random fractal sets. A complementary way is to endow two subintervals with exactly one-half of the measure but to choose their *lengths* randomly [8]. The analysis of these random length models is undertaken in Appendix A. The results are very similar to those of random measure models. The conclusion will be that it is the correlation between levels, rather than the detailed refinement process, that determines the gross structure of the scaling spectrum.

A. No correlation

In this case we take the numbers x_i to be completely independent. Then the simultaneous probability distribution factorizes

$$P(x_1, \dots, x_n) = P(x_1) \cdots P(x_n). \quad (12)$$

We take the distributions $P(x_i)$ to be uniform on the unit interval for all i . The product $p_{n,j}^q = r_1^q \cdots r_n^q$ involves factors x_i^q and $(1-x_i)^q$, which have identical expectation values

$$\langle x^q \rangle = \int_0^1 x^q dx = \frac{1}{q+1} = \int_0^1 (1-x)^q dx = \langle (1-x)^q \rangle, \quad (13)$$

where x denotes any of the x_i 's. Using this symmetry result and Eq. (12) we obtain for each averaged member $\langle p_{n,j}^q \rangle$ of the partition sum the simple j -independent expression

$$\langle p_{n,j}^q \rangle = \left(\frac{1}{q+1} \right)^n. \quad (14)$$

Therefore,

$$\sum_{j=1}^{2^n} \langle p_{n,j}^q \rangle = \left(\frac{2}{q+1} \right)^n. \quad (15)$$

Substitution of Eq. (15) into Eq. (9) yields, irrespective of the value of n ,

$$\tau(q) = -1 + \log_2(q+1), \quad (16)$$

with the companion spectrum $f(\alpha)$ of scaling exponents given by

$$f(\alpha) = 1 - \alpha + \frac{1}{\ln 2} (1 + \ln \alpha + \ln \ln 2) \quad (17)$$

and drawn in Fig. 2. For $\alpha \downarrow 0$ we have $f(\alpha) \sim \ln \alpha$, while for $\alpha \rightarrow \infty, f(\alpha) \sim -\alpha$. The spectrum is negative for small and large α values and positive for intermediate values. The absence of correlation between successive refinement levels leads to the absence of the n dependence of $\tau(q)$ and $f(\alpha)$. A similar cascade but with discrete probabilities has been given in [9].

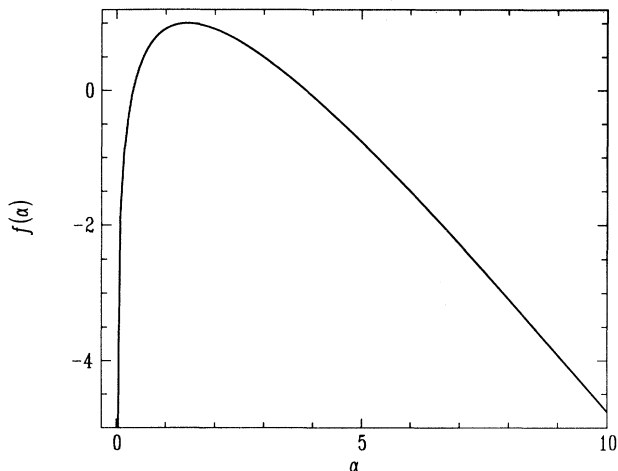


FIG. 2. Scaling function $f(\alpha)$ of a binary random multiplicative process without correlation between successive refinement steps.

B. Self-averaging

The scaling functions of Eqs. (16) and (17) are the result of ensemble averaging. An infinite product $p_{n,j}^q = r_1^q r_2^q \cdots r_n^q$ with randomly chosen values x_i is already an average in itself. The question is if this “self-average” is the same as ensemble averaging. Self-averaging implies that instead of Eq. (8), the expression

$$\Gamma_n(q, \tau) = 2^{n\tau} \sum_{j=1}^{2^n} p_{n,j}^q = 1 \quad (18)$$

is used to obtain $\tau_n(q)$. Because of the special structure of the $p_{n,j}$ we have

$$\sum_{j=1}^{2^n} p_{n,j}^q = \prod_{i=1}^n [x_i^q + (1-x_i)^q]. \quad (19)$$

Taking logarithms in Eq. (18) we find

$$\tau_n(q) = -\frac{1}{n} \sum_{i=1}^n \log_2 [x_i^q + (1-x_i)^q]. \quad (20)$$

Since the x_i are independently drawn from the same uniform distribution, the right-hand side of Eq. (20) can, in the limit $n \rightarrow \infty$, be viewed as the averaging of $\log_2 [x_i^q + (1-x_i)^q]$ over the levels of the cascade. Self-averaging thus leads to the expression

$$f_n(\alpha) = \begin{cases} f(\alpha) + \frac{2}{n} + \frac{1}{n \ln 2} [1 + \ln \ln 2 + \ln \alpha], & 0 < \alpha < 1 \\ f(\alpha) + \frac{1}{2n \ln 2} [1 + \ln(2 \ln 2) + \ln(\alpha - 1) + \ln \pi], & \alpha > 1. \end{cases} \quad (27)$$

For finite n , therefore, the function $f_n(\alpha)$ can take on negative values. The $f_n(\alpha)$ spectrum is drawn in Fig. 3 for several n values. The convergence of $f_n(\alpha)$ to $f(\alpha)$ is $O(1/n)$ and thus slow. At finite resolution one might

$$\tau(q) = - \int_0^1 \log_2 [x^q + (1-x)^q] dx. \quad (21)$$

The resulting $f(\alpha)$ is nowhere negative and symmetrical around the point $\alpha = 1/\ln 2$. Therefore, self-averaging is essentially different from ensemble averaging.

C. Complete correlation

In this case the x_i 's are identical $x_1 = x_2 = \cdots = x_n$. At all levels one and the same stochastic variable, say, x , is used. The simultaneous probability distribution $P(x_1, \dots, x_n)$ degenerates to a univariate distribution $P(x)$, for which we again take the uniform distribution on the unit interval. The partition sum in Eq. (6) can be written as

$$\sum_{j=1}^{2^n} p_{n,j}^q = [x^q + (1-x)^q]^n. \quad (22)$$

Ensemble averaging leads to the integral

$$\left\langle \sum_{j=1}^{2^n} p_{n,j}^q \right\rangle = I_n(q) = \int_0^1 [x^q + (1-x)^q]^n dx. \quad (23)$$

For large n reliable approximations for this integral can be derived by expanding the factor $[x^q + (1-x)^q]$ around the value of x where the integrand reaches a maximum. The analysis is explicated in Appendix B and its result is

$$\tau_n(q) = \begin{cases} \tau(q) + \frac{1}{n}(\log_2 q - 1) + \frac{1}{n} \log_2 n, & q > 1 \\ \tau(q) + \frac{1}{2n} \log_2 [q(1-q)/\pi] + \frac{1}{2n} \log_2 n, & 0 < q < 1 \end{cases} \quad (24)$$

with

$$\tau(q) = \lim_{n \rightarrow \infty} \tau_n(q) = \begin{cases} 0, & q > 1 \\ q - 1, & 0 < q < 1. \end{cases} \quad (25)$$

In the limit of infinite refinement, therefore, the function $\tau(q)$ is no longer differentiable at the point $q = 1$ and exhibits a *phase transition* phenomenon. The companion spectrum of scaling exponents

$$f(\alpha) = \min_q \{q\alpha - \tau(q)\} = \begin{cases} \alpha, & 0 < \alpha < 1 \\ 1, & \alpha > 1 \end{cases} \quad (26)$$

is piecewise linear and always positive. At any *finite* n , $f_n(\alpha)$ can be found from the continuous Legendre transformation of Eq. (24),

therefore be easily misled to conclude the presence of negative dimensions. These negative dimensions are merely finite-size artifacts.

An important conclusion from the present analysis is

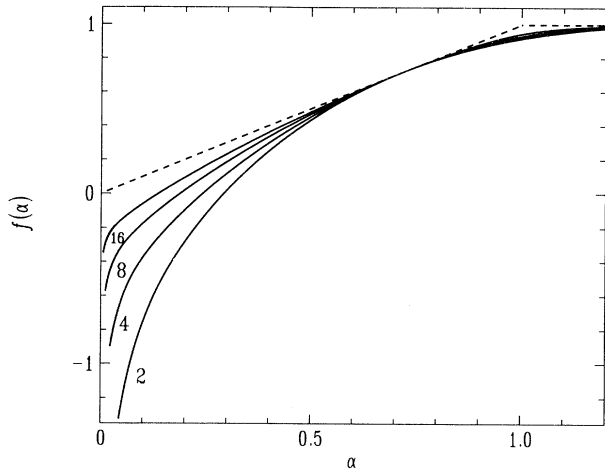


FIG. 3. Scaling functions $f_n(\alpha)$ of a binary random multiplicative process with complete correlation between successive refinement steps. Solid lines, number of refinement steps ranging from $n = 2$ to $n = 16$; dashed line, asymptotic scaling function ($n \rightarrow \infty$). The asymptotic scaling function shows a phase transition phenomenon.

that for large n the function $\tau_n(q)$ takes on the form

$$\tau_n(q) = \tau(q) + \frac{1}{n}K_1(q) + \frac{\log_2 n}{n}K_2(q). \quad (28)$$

Nonzero functions $K_1(q)$ and $K_2(q)$ are the consequence of nonvanishing correlations between refinement levels. For the present case $K_1(q) = \log_2 q - 1$, and $K_2(q) = 1$ for $q > 1$. We will demonstrate that these functional forms that correspond to the case of complete correlation are “maximal.” In the case of only partial correlation, the corresponding functions are at a given value of q always smaller than the present functions.

The scaling functions $\tau_n(q)$ are only defined for $q > 0$. Consequently, the complementary scaling function $f(\alpha)$ is only defined to the left of its maximum. One-sided scaling functions are also found in the description of clusters that are grown by diffusion limited aggregation [10].

D. Finite correlation depth

In this case we introduce a simultaneous probability distribution that will lead to an exponentially decaying correlation function. The essential idea is to make use of the equality

$$P(x_1, \dots, x_n) = P(x_n | x_1, \dots, x_{n-1})P(x_1, \dots, x_{n-1}). \quad (29)$$

with $P(x_n | x_1, \dots, x_{n-1})$ the conditional probability distribution of x_n given the values of x_1, \dots, x_{n-1} . We assume that each x_i is only conditioned on the preceding x_{i-1} . This Markovian condition can be expressed as

$$P(x_i | x_1, \dots, x_{i-1}) = P(x_i | x_{i-1}). \quad (30)$$

Applying Eqs. (29) and (30) repeatedly we find

$$P(x_1, \dots, x_n) = P(x_1)P(x_2 | x_1) \cdots P(x_n | x_{n-1}). \quad (31)$$

This form is extremely appropriate to calculate the ensembleaveraged partition sums $\sum_{i=1}^{2^n} \langle p_{n,j}^q \rangle$ in Eq. (9). We illustrate this for one term in the summation in Eq. (9), namely, the one corresponding to $j = 1$

$$p_{n,1} = x_1 x_2 \cdots x_n. \quad (32)$$

Its average is given by

$$\begin{aligned} \langle p_{n,1}^q \rangle &= \int_0^1 dx_1 x_1^q P(x_1) \int_0^1 dx_2 x_2^q P(x_2 | x_1) \cdots \\ &\times \int_0^1 dx_n x_n^q P(x_n | x_{n-1}). \end{aligned} \quad (33)$$

Simple recursion rules for the computation of ensembleaveraged partition sums result if we take the conditional probability $P(x_i | x_{i-1})$ to be a piecewise constant function. To this aim we cover the unit interval with a grid of points k/m , $k = 0, \dots, m$, that define intervals with length $1/m$. The normalized conditional probability is then given in terms of this grid

$$P(x_i | x_{i-1}) = \begin{cases} m - \delta & \text{if } x_i \text{ and } x_{i-1} \\ & \text{are in the same interval} \\ \gamma = \frac{\delta}{m-1} & \text{otherwise} \end{cases} \quad (34)$$

for some parameter δ with $0 \leq \delta \leq m - 1$. The function $P(x_i | x_{i-1})$ is sketched in Fig. 4 for $m = 64$, $x_{i-1} = 20/64$, and $\delta = 32$.

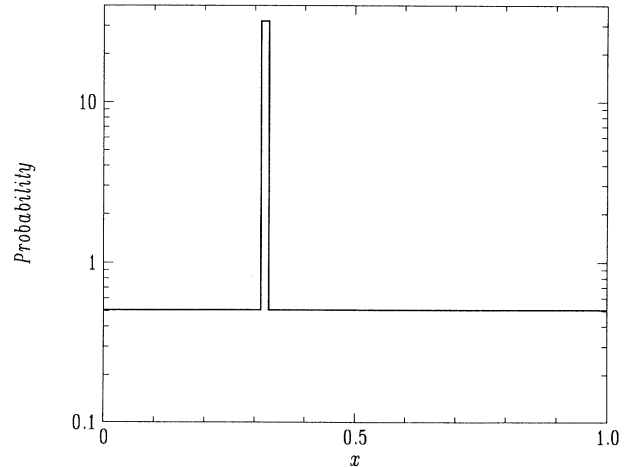


FIG. 4. Conditional probability function $P(x_i | x_{i-1})$ for a given x_{i-1} . Probability functions of this form lead to a cascade with an exponentially decaying correlation function of the multipliers at successive refinement steps. The conditional probability function is piecewise constant on intervals of length $1/m$. Shown is the case $m = 64$, $\delta = 32$, where x_{i-1} is in the interval $[20/64, 21/64]$. The number δ determines the height of the spike. The height increases with decreasing δ .

At the first level the variable x_1 is selected according to a uniform distribution on $[0, 1]$. In the case $\gamma = 0$, all $x_i, i = 2, \dots, n$, are uniformly randomly chosen in the subinterval with index $[mx_{i-1}]$, where the square brackets denote the integer part. In the case $\gamma > 0$, the variable x_i has also a nonzero probability γ to be outside the interval $[mx_{i-1}]$. In Appendix C we prove that the correlation function for this model is

$$C(1, i) = \begin{cases} 1 & \text{if } i = 1 \\ \left(1 - \frac{1}{m^\gamma}\right) \exp[-(i-1)/\xi] & \text{if } i > 1, \end{cases} \quad (35)$$

where the correlation depth $\xi = -1/\ln(1 - \gamma)$. The correlation depth is zero for $\gamma = 1$ (i.e., $\delta = m - 1$) and is infinite for $\gamma = 0$ ($\delta = 0$). The last case is equivalent to the completely correlated model of Sec. II C in the limit $m \rightarrow \infty$. Therefore this model displays a continuous transition between the case of completely *dependent* multipliers x_i and the case of completely *independent* multipliers. In Appendix D we derive a recursion rule for the ensemble-averaged partition sum that can be readily implemented on a computer.

Figure 5 compares the dimension spectrum $f(\alpha)$ for the correlation depths $\xi = 3.413\dots$ and $\xi = 1.413\dots$ ($m = 64, \delta = 16$ and $m = 64, \delta = 32$, respectively) with the corresponding spectra for the completely correlated case and the case of uncorrelated multipliers. The convergence of the correlated case is shown by overlaying the graphs with different n . Evidently, the $f(\alpha)$ functions of the correlated cases are intermediate between the extremes of uncorrelated and completely correlated multipliers. The negative dimensions are genuine and are

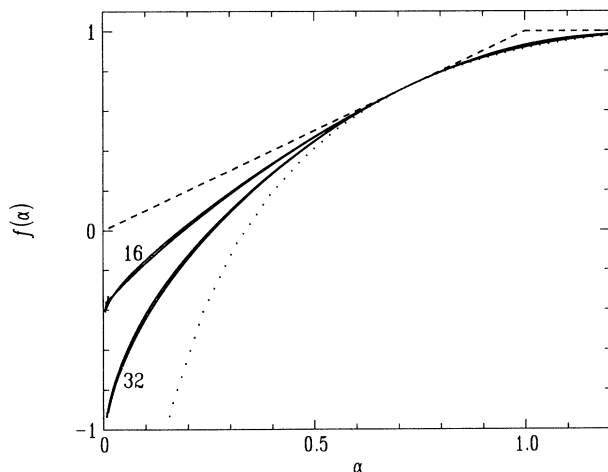


FIG. 5. Solid lines, scaling function of a binary cascade with nonzero correlations between successive refinement steps. The correlation depths are $\xi = 1.413$ and $\xi = 3.413$ for $\delta = 32$ and $\delta = 16$, respectively. The value of δ is indicated. The number δ controls the shape of the conditional probability function. The strength of correlations increases with decreasing δ . The convergence with increasing number of cascade steps is demonstrated by overlaying curves computed from $n = 3, 4, 5$ and $n = 4, 8, 16$ for each δ . Dashed line, cascade with infinite correlation depth (Fig. 3); dotted line, cascade with zero correlation depth (Fig. 2).

not due to finite size effects.

For a fine cover of the unit interval (large m) and for $\gamma = 0$, the model of this section is the same as the model treated in Sec. II C. Therefore, we expect that both models have the same large n behavior Eq. (28). We have found that this is indeed approximately true. The functions $K_1(q)$ and $K_2(q)$ are shown in Fig. 6 for $m = 64$ and values of ξ ranging from $\xi = 16$ to $\xi = 2$. They were computed by linearly solving for K_1, K_2 , and τ from $\tau_n(q)$ at three values of n . For Fig. 6 we used $n = 3, 4$, and 5 ; larger values of n produced results that were only slightly different from those shown. At a given value of q , $K_1(q)$

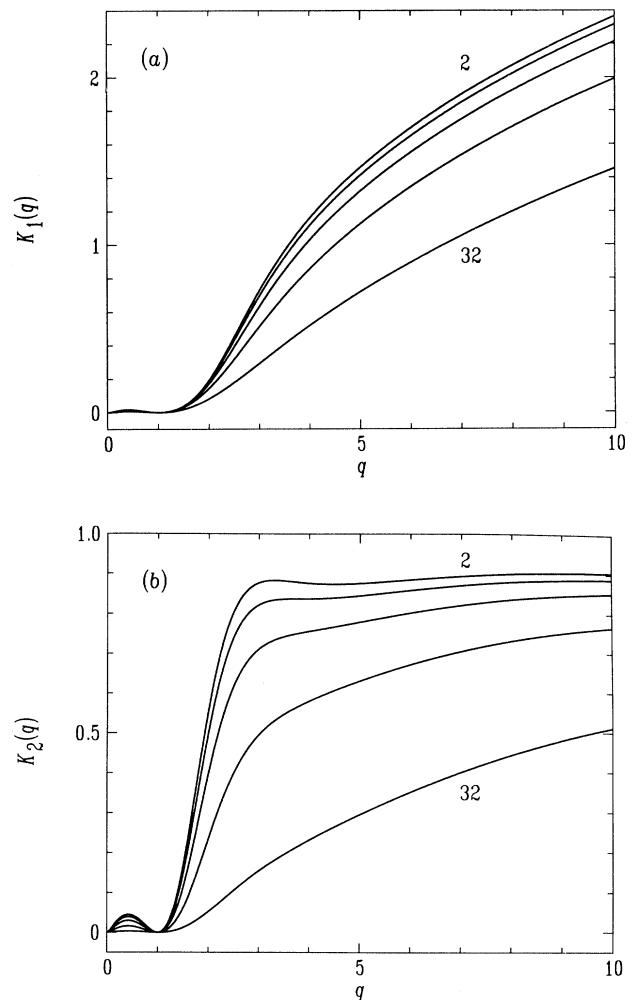


FIG. 6. Correction functions for cascades with intermediate correlation between successive refinement steps. The correction functions are defined in the asymptotic form of the scaling function as $\tau_n(q) = \tau(q) + K_1(q)/n + K_2(q) \log_2(n)/n$. The indicated number δ controls the shape of the conditional probability function. The strength of correlations increases with decreasing δ . The value of δ is 2, 4, 8, 16, 32, respectively. The correlation depth ranges from $\xi = 1.4$ for $\delta = 32$ to $\xi = 15$ for $\delta = 2$. (a) The function $K_1(q)$ that multiplies the $1/n$ term in the expression for $\tau_n(q)$. (b) The $K_2(q)$ that multiplies the $\log_2(n)/n$ term.

and $K_2(q)$ are seen to *decrease with decreasing correlation depth* ξ . It also appears that at a fixed value of q , the function $K_1(q)$ approaches the maximally correlated case as $K_{1,\xi=\infty} - K_1(q) \sim 1/\xi$.

In the binary cascades considered so far, random multipliers in a given ensemble member were induced by drawing a single random number x_n at each level n . For turbulence, a more realistic procedure would be to draw 2^{n-1} random numbers at each level n . Numerical simulations have shown that this procedure gives rise to scaling functions $\tau(q)$ that for $q > 0$ are indistinguishable from the scaling functions that are derived in Sec. II.

III. MEASURING MULTIPLIERS

Multipliers of turbulent dissipation at base a are measured by dividing intervals of length l_1 into a daughter intervals of length $l_2 (= l_1/a)$ and computing the histogram $P^{(a)}(m)$ of ratios $m_i = \epsilon_i(l_2)/\epsilon(l_1)$, $i = 1, \dots, a$, where $\epsilon_i(l_2)$ is the integrated dissipation over the i th daughter interval. In the models discussed so far, the value of the base was restricted to powers of 2, $a = 2^n$.

It follows from Eq. (4) that the scaling function $\tau_a(q)$ is defined in terms of the moments of the multiplier distribution function

$$\tau_a(q) = -1 - \frac{1}{\log a} \log \left(\int_0^\infty x^q P^{(a)}(x) dx \right). \quad (36)$$

As demonstrated in Eq. (3), if the dissipation has scaling behavior and if the multipliers x at different levels are uncorrelated, the function $\tau(q)$ does not depend on a . On the other hand, if the multipliers of subsequent levels are correlated, the function $\tau_a(q)$ will have an a dependence.

The function $\tau(q)$ is nothing else but the logarithm of the Mellin transform $M[P^{(a)}]$ of the distribution of multipliers $P^{(a)}(x)$. This transform is defined as

$$M[P](z) = \int_0^\infty P(x) x^{z-1} dx; \quad (37)$$

therefore

$$\tau_a(q) = -1 - \frac{1}{\log a} \log M[P^{(a)}](q+1). \quad (38)$$

Now consider a cascade with a division into a^2 intervals. It can be considered as level 2 of a cascade with base a , but also as level 1 of a cascade with base a^2 . Both views must lead to the same function $\tau(q)$. The relation between the two probability distribution functions $P^{(a)}$ and $P^{(a^2)}$ is given by

$$P^{(a^2)}(z) = \int_0^1 \frac{1}{x} P^{(a)}(z/x) P^{(a)}(x) dx. \quad (39)$$

The Mellin transforms of the distribution functions in such a convolution are related as

$$M[P^{(a^2)}] = \left(M[P^{(a)}] \right)^2. \quad (40)$$

Base independence of the scaling functions $\tau_a(q)$ therefore implies a special relation between the distribution functions corresponding to different values of the base. For the model without correlation in Sec. II A, it can easily be shown that if $P^{(2)}(x)$ is uniform,

$$P^{(2^n)}(x) = \frac{1}{n!} (-\ln x)^n. \quad (41)$$

On the other hand, for the completely correlated case of Sec. II C, the distribution function at level n is determined by the singularities that result from mapping a uniform distribution of points on the unit interval through the functions $x^k(1-x)^{n-k}$, $k = 1, \dots, n$.

The scaling functions $\tau(q)$ and the associated distribution functions of multipliers are two complementary descriptions of the scaling properties of the turbulent dissipation field. Because the scaling functions for increasing q are determined by the increasingly higher moments of the distribution functions, the statistical accuracy of the distribution functions determines the accuracy of $\tau(q)$ at large q or the accuracy of $f(\alpha)$ at values of α where it is most negative.

If multipliers of the turbulent dissipation field at different bases a are correlated, the measured function $\tau_a(q)$ will depend on the base a . It is demonstrated in Sec. II D that for the binary (2^n -based) cascades considered there, the large n behavior of $\tau_n(q)$ is determined by terms proportional to $1/n$ and $(\log_2 n)/n$. We expect that in complete analogy the large a behavior of $\tau_a(q)$ is approximately determined by terms proportional to $1/\log a$ and $\log(\log a)/\log a$. For convenience we will retain only the first term in which case the function $\tau(q)$ can be estimated from a measurement at two bases a_1 and a_2 ,

$$\tau(q) = \frac{\tau_{a_1}(q) \log a_1 - \tau_{a_2}(q) \log a_2}{\log a_1 - \log a_2}. \quad (42)$$

We will use this expression when analyzing the results of a turbulence experiment.

IV. EXPERIMENTAL RESULTS

In order to test for the existence of $\log a$ corrections in the analysis of the scaling properties of the turbulent dissipation field we have performed a laboratory turbulence experiment. The Reynolds number in this experiment is modest, $R_\lambda = 8 \times 10^2$, as based on the Taylor microscale λ . A turbulent flow emanated with a mean velocity of 30 m/s from a jet (0.12 m diameter). Velocity fluctuations were measured 2.6 m downstream where the mean velocity was 11.7 m/s and the turbulent fluctuations had a rms size of 2.3 m/s. Using a standard hot-wire probe of size 0.2 mm, a modest number (5×10^7) of velocity samples was registered and stored. The length of the time series was approximately 4×10^5 integral scales L . The 12-bit data were acquired with a 33-kHz sampling rate and using a four-pole antialiasing filter at 16.5 kHz. The dissipation length scale was $\eta = 8.7 \times 10^{-5}$ m and the Taylor microscale that gauges the extent of correlations in the flow was $\lambda/\eta = 57$.

In the case that the velocity fluctuations are much smaller than the mean flow velocity, a time signal from a stationary probe can be interpreted as a spatial signal on a line that cuts through the turbulent velocity field [11]. We assumed that this applies to our experiment.

Although the Reynolds number is modest, the velocity increments of the turbulent fluctuations have a clear scaling behavior that stretches over nearly two decades. This is demonstrated in Fig. 7, which shows the third-order structure function $G_3(r) = \langle [u(x+r) - u(x)]^3 \rangle$ as a function of r . In the case of homogeneous and isotropic turbulence, the scaling part of G_3 must behave as $G_3(r) \sim r$ [12]. We find that $G_3(r) \sim r^\zeta$, with $\zeta = 1.03$, which is slightly but significantly larger than 1.

The dissipation ϵ is a sum of derivatives $\epsilon = \nu \sum_{i,j}^3 (\partial u_i / \partial x_j)^2$ of which we measure the term $(\partial u_1 / \partial x_1)^2$ by time differentiation of the measured signal. In the case of isotropic turbulence, $\langle \epsilon \rangle = 15\nu \langle (\partial u_1 / \partial x_1)^2 \rangle$. As is customary, we assume this relation to hold also for the instantaneous quantities.

Figure 8 shows distribution functions of multipliers m that were measured by computing the ratio $m = \epsilon(l/a) / \epsilon(l)$ for $l/\eta = 570$ and $a = 2, 3, \dots, 9$. The histograms were accumulated by dividing the measured time series into 2×10^5 intervals of length l .

The average correlation between the value of the multiplier at distance l and that at distance al with $a = 2$ is shown in Fig. 9. The correlation function demonstrates the importance of the Taylor microscale (here $\lambda/\eta = 57$) where it has a minimum. Multipliers of subsequent refinements at smaller distances $l < \lambda$ become increasingly correlated. It is expected therefore that the range over which the scaling function $\tau(q)$ is l independent is bounded from below by the Taylor microscale rather than by the dissipation scale. Therefore, the scaling dynamical range of multiplier distributions will be smaller than the scaling range of the velocity increments that is shown

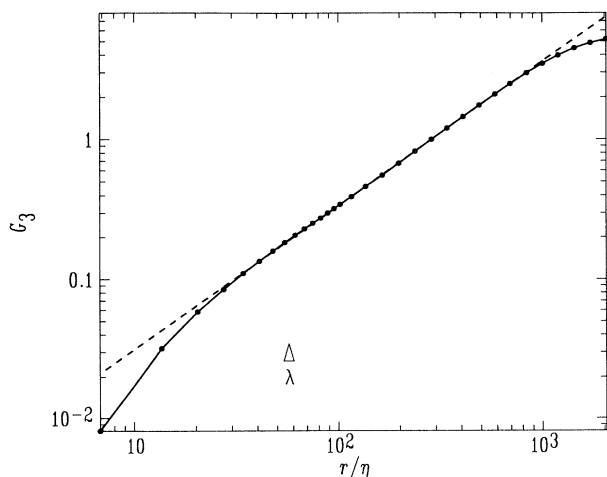


FIG. 7. Measured third-order structure function $G_3(r)$ as a function of r/η in jet turbulence. Dashed line, fit of $G_3(r) \simeq r^\zeta$ with $\zeta = 1.03$. The scaling range extends approximately from $r/\eta = 30$ to $r/\eta = 10^3$. The arrow points to the Taylor microscale.

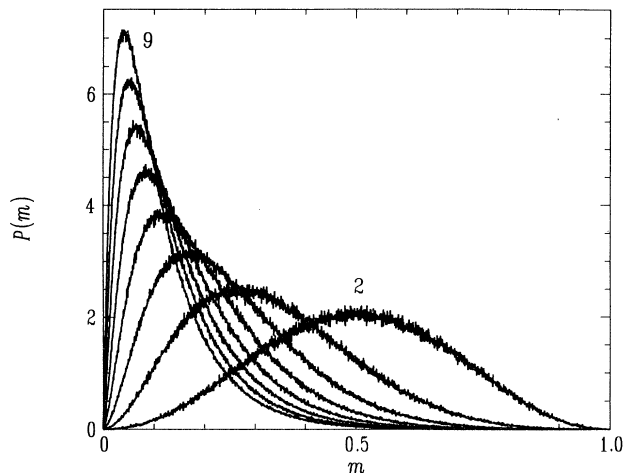


FIG. 8. Measured multiplier distributions of turbulent dissipation in a jet flow. The multipliers m are $m = \epsilon(r) / \epsilon(r/a)$, where $r/\eta = 570$ and the base a takes the values $a = 2, 3, \dots, 9$, respectively.

in Fig. 7. A similar behavior is shown by the correlation between the multiplier $m = \epsilon(l/a) / \epsilon(l)$, $a = 2$, and the mother-interval dissipation $\epsilon(l)$.

The correlation functions of Fig. 9 were measured for the situation that the daughter interval was centered in the mother interval. It is well known that the correlation depends on the relative location of both intervals [6]. This relative location is expressed in terms of the homogeneity parameter h

$$h = \frac{x - x'}{l(1 - 1/a)}, \quad (43)$$

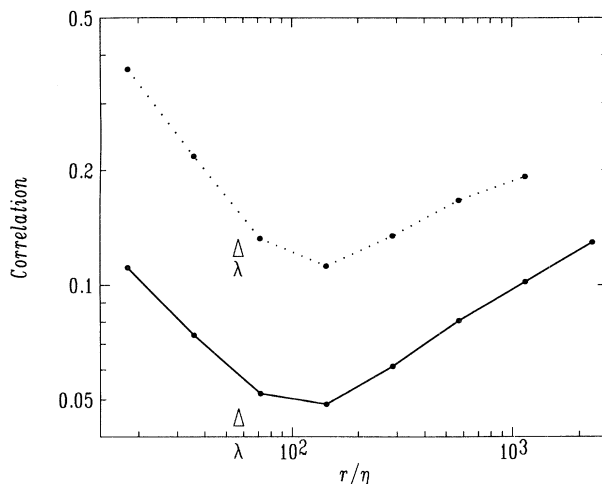


FIG. 9. Correlation between multipliers at successive refinement steps and between multipliers and mother interval dissipation measured in a turbulent jet using refinements with base $a = 2$. Dots connected by a dotted line, correlation between multipliers at r and ra ; dots connected by full line, correlation between multiplier and mother interval dissipation at level r . The correlation functions show a minimum at approximately the Taylor microscale ($\lambda/\eta = 57$). The arrow points to λ .

where x and x' are the centers of the mother interval, here with length la and a daughter interval with length l , respectively. The value of h ranges from $-1/2$ to $1/2$ with the centered daughter interval at $h = 0$. Figure 10 shows the h dependence of the (m, ϵ) correlation as a function of h for a range of bases a . The correlation function is strongly inhomogeneous and shows a marked asymmetry. We believe that this asymmetry is significant; it perhaps points to deviations from the frozen turbulence hypothesis. Clearly, the inhomogeneous nature (i.e., h dependence) of correlations and their scale (l) dependence is not accounted for in our cascade models.

Our central experimental result is the approximate validity of Eq. (5) to describe the asymptotic self-similarity of multiplier distributions of turbulent dissipation. It is demonstrated in Fig. 1, which shows the scaling functions measured at $l/\eta = 570$. Figure 1 also shows good agreement with the results of Ref. [3] that were obtained in the atmospheric boundary layer. The correction function $K(q)$ was obtained from measured $\tau_a(q)$ at $a = 2, 4$. Figure 11 shows the function $K(q)$ and compares it to one obtained from scaling functions at $a = 2, 8$. The results demonstrate that the asymptotic self-similarity of turbulence is, to a good approximation, described by Eq. (5).

In the case of strict self-similarity in the inertial range, the scaling functions $\tau_a(q)$ should not depend on the inertial-range scale l (cf. the length of the mother interval) where they are measured. Probably because our Reynolds number is modest ($R_\lambda = 8 \times 10^2$), we have found a significant variation of $\tau_a(q)$ with l . This is demonstrated in Fig. 12, which shows the variation of $f(\alpha)$ that was computed from measured $\tau_a(q)$ at $a = 2$ and l ranging from $l/\eta = 1150$ to $l/\eta = 72$. The l dependence that we find agrees with results by Van Atta and Yeh [6] obtained in atmospheric boundary layer flows, but it disagrees with those of Chhabra and Sreenivasan

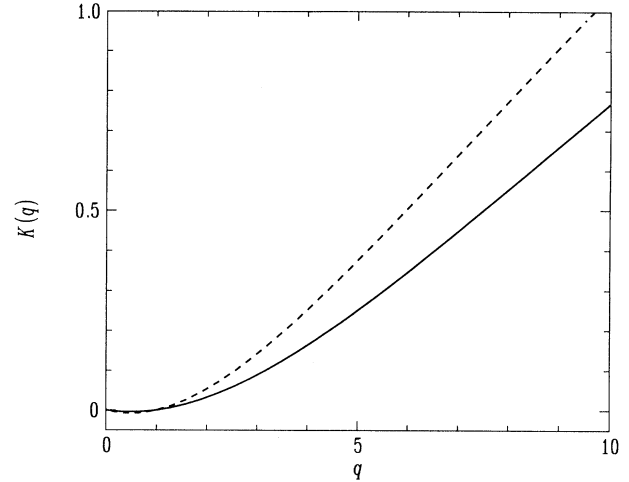


FIG. 11. Correction function $K(q)$ defined in $\tau_a(q) = \tau(q) + K(q)/\ln a$, measured in a turbulent jet flow at $r/\eta = 570$ at $a = 2, 4$ (solid line) and $a = 2, 8$ (dashed line). This function is used to correct for finitesize effects in $f(\alpha)$ due to correlations between multipliers.

[3] which were also obtained in an atmospheric boundary layer but show scale *independent* multiplier distributions. The results of Fig. 1 were obtained for a value of l in the middle of the inertial range shown in Fig. 7.

The scaling range of multiplier experiments is smaller than the inertial range of structure functions as it is bounded from below by the Taylor microscale. Because the inertial range widens with increasing Reynolds number, we expect to reach the scale independence of $\tau(q)$ at much larger values of R_λ . This is clearly a point of further research.

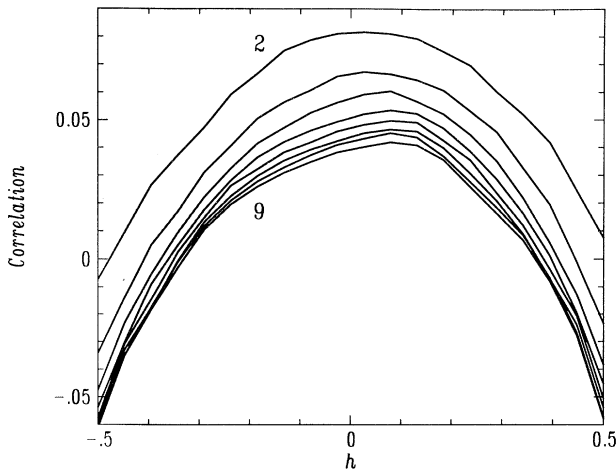


FIG. 10. Dependence of the correlation between multiplier $\epsilon(r)/\epsilon(r/a)$ and mother dissipation $\epsilon(r)$ on the relative position of the r/a subinterval at $r/\eta = 570$ and base a ranging from $a = 2$ to $a = 9$.

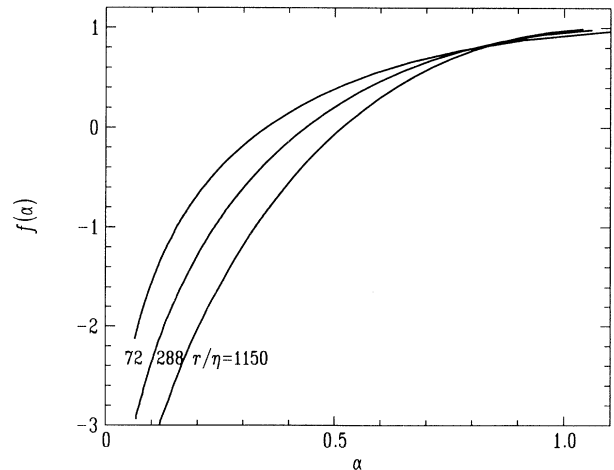


FIG. 12. Scale dependence of $f(\alpha)$ that was measured in a turbulent jet experiment. The scaling function $f(\alpha)$ was determined from multipliers at base $a = 2$ and scales l , $l/\eta = 1150, 580, \text{ and } 72$, respectively.

V. CONCLUDING REMARKS

Multifractals provide a rich framework to analyze turbulent fluctuations. Clearly, turbulence gives rise to *random* fractals and one may expect fractal dimensions of proper long-time averages to become *negative*. A key result of our work is that due to the presence of correlations, the scaling behavior of these fractals is often only *asymptotic*. Incidentally, the existence of logarithmic preasymptotic factors is a severe impairment of a scaling approach to multiplier distributions.

We do not claim to have designed cascade models for turbulence. The purpose of our models has been to demonstrate the effect of correlations on scaling. However, an obvious conclusion is that multiplier correlations in turbulence are not complete as for the model of Sec. IIC [13].

A quite subtle problem in the interpretation of experimentally measured dissipation in terms of multipliers m_i is that the numbers m_i must satisfy the trivial normalization condition $\sum_{i=1}^a m_i = 1$. The form of measured multiplier distribution functions $P^{(a)}(m)$ is determined both by this normalization condition and by self-similarity that relates $P^{(a)}(m)$ and $P^{(b)}(m)$ through their Mellin transforms. As seen in Fig. 8, the maximum of $P^{(a)}(m)$ shifts to smaller m when a increases. This shift is due to the satisfaction of the normalization condition. The normalization requirement induces correlations between m_1, \dots, m_a at a given level. These correlations should be distinguished from the level to level correlations that are considered in this paper. We have found it (numerically) perfectly possible to construct self-similar cascades whose multipliers satisfy the normalization condition [14].

Measuring turbulent scaling through multipliers implies averages over many realizations of a fractal process and the question of statistical accuracy is as important as in the case of high-order structure functions. Convergence of high moments of the multiplier distribution requires the accumulation of very long time series. The advantage of the multiplier approach is that the convergence problems are explicit. The question of statistical convergence is much harder to deal with in the standard approach where an average over scaling functions is taken.

Of course, the measurement of time series in a single point provides only very limited information about the turbulent flow field. An obvious extension is the simultaneous measurement of velocity fluctuations in many points of the flow field. These measurements and their interpretation in terms of scaling functions are a goal of current research.

ACKNOWLEDGMENTS

The authors thank Mogens Jensen for introducing them to the example treated in Sec. III. They also thank Sjoerd Rienstra for deriving the integrals in Appendix B. This work is also part of the Stichting voor Fundamenteel Onderzoek der Materie, which is financially supported by the Nederlandse Organisatie voor Wetenschappelijk Onderzoek.

APPENDIX A: RANDOM SCALES

In [8] a multifractal is studied with a deterministic, trivial redistribution of the probability and a stochastic refining of the intervals. Here we briefly show that also in this case the correlation between successive refinement steps crucially determines the $\tau(q)$ and $f(\alpha)$ scaling functions. At each refinement level n two stochastic variables x_n and y_n are introduced with $x_n, y_n \geq 0$ and $x_n + y_n \leq 1$. Each interval at level n is divided into two smaller ones of lengths x_n and y_n . The measure of the mother interval is distributed equally over the daughter intervals. At level n the fractal thus consists of 2^n intervals, which all together cover a fraction of the unit interval and each interval has measure 2^{-n} . The partition function is given by

$$\Gamma(q, \tau) = 2^{-nq} \sum_j l_{n,j}^{-\tau}, \quad (\text{A1})$$

with $l_{n,j}$ the length of the j th interval at level n . We have

$$l_{n,j} = r_1 r_2 \dots r_n \quad (\text{A2})$$

with $r_i = x_i$ or $r_i = y_i$, $i = 1, \dots, n$. To obtain the scaling function $\tau(q)$ the averages $\langle l_{n,j}^{-\tau} \rangle$ must be calculated. They are determined by a joint probability distribution $P(x_1, y_1, \dots, x_n, y_n)$. To show the strong relation between the correlation structure and the scaling exponents, we consider the case where the r_i from different levels are independent and, at the other extreme, the case where the r_i are the same for each level.

We first deal with the case, not treated in [8], that x_i and $x_{i'}$, on the one hand, and y_i and $y_{i'}$, on the other hand, are uncorrelated for different i and i' . Here the relevant distribution function is $P(x_i, y_i)$. The probabilities are taken independent of i and uniformly distributed on the triangle $x_i, y_i \geq 0$ and $x_i + y_i \leq 1$. From the symmetry between x_i and y_i we conclude that

$$\langle (r_1 r_2 \dots r_n)^{-\tau} \rangle = \langle x_1^{-\tau} \rangle^n, \quad (\text{A3})$$

which is easily calculated:

$$\langle x_1^{-\tau} \rangle = 2 \int_0^1 dx_1 x_1^{-\tau} \int_0^{1-x_1} dy_1 = \frac{2}{(1-\tau)(2-\tau)}. \quad (\text{A4})$$

It leads to the restriction $\tau < 1$. The averaged partition function is thus given by

$$\langle \Gamma_n(q, \tau) \rangle = 2^{n(2-q)} [(1-\tau)(2-\tau)]^{-n}. \quad (\text{A5})$$

Equating this expression to unity we find that the scaling exponents are independent of n and given by

$$\begin{aligned} \tau(q) &= \frac{3}{2} \left\{ 1 \pm \left[1 - \frac{8}{9} (1 - 2^{1-q}) \right]^{1/2} \right\} \\ &\approx \frac{3}{2} \left(1 - 2^{\frac{1-q}{2}} \right). \end{aligned} \quad (\text{A6})$$

In the last line we made a small approximation and chose the minus sign that corresponds to positive α . The cor-

responding $f(\alpha)$ spectrum is

$$f(\alpha) = -\frac{3}{2} + \alpha \left\{ 1 + \frac{2}{\ln 2} \left[1 - \ln \alpha + \ln \left(\frac{3}{4} \ln 2 \right) \right] \right\}. \quad (\text{A7})$$

The spectrum of dimensions is negative for small and large values of α . It is similar to the dimension spectrum for the case of random *measure* refinements that is treated in Sec. II A.

The case of complete correlation between levels is treated in [8]. In this case we set $x_i = x$ and $y_i = y$, $i = 1, \dots, n$. The probability distribution $P(x, y)$ is uniform on the triangle $x, y \geq 0$, $x + y \leq 1$. The averaged partition function is given by

$$\langle \Gamma_n(q, \tau) \rangle = 2^{-qn} I_n(q, \tau), \quad (\text{A8})$$

with the integral $I_n(q, \tau)$ defined as

$$I_n(q, \tau) = \int_0^1 dx \int_x^1 dy (x^{-\tau} + y^{-\tau})^n. \quad (\text{A9})$$

From the condition

$$\langle \Gamma_n(q, \tau) \rangle = 1, \quad (\text{A10})$$

an implicit equation for the scaling exponent $\tau_n(q)$ is obtained. The evaluation of the integral $I_n(q, \tau)$ is intricate and several cases have to be investigated carefully. For $\tau \geq 0$ (i.e., $q > 1$) the integrand reaches a maximum in $(x, y) = (0, 0)$ and the integral diverges unless $\tau < 1/n$. So, in the limit $n \rightarrow \infty$ we have $\tau = 0$, $q > 1$. For $-1 < \tau < 0$ (i.e., $0 < q < 1$) the integrand reaches a maximum $2^{n(\tau+1)}$ in $(x, y) = (1/2, 1/2)$. Expansion of the integrand around this maximum up to first order results in the relation

$$2^{n[\tau+1-q+\frac{1}{n} \log_2(-\delta/n\tau)]} = 1, \quad (\text{A11})$$

where δ is an arbitrary, positive number, $\delta \ll 1$. From this we conclude that

$$\tau_n(q) = \tau(q) + \frac{1}{n \ln 2} [\ln n(1-q) - \ln \delta] \quad (\text{A12})$$

with

$$\tau(q) = q - 1. \quad (\text{A13})$$

Therefore, this model has the same asymptotic $f(\alpha)$ spectrum as the model of Sec. II C, where we have kept the scales fixed but have randomly distributed the measure.

For $\tau < -1$ (i.e., $q < 0$) the integrand reaches a maximum value of 1 in $(x, y) = (1, 0)$. Expansion of the integrand around this maximum up to first order results in

$$\tau_n(q) = -\frac{1}{n} 2^{qn/2+1}. \quad (\text{A14})$$

We note that Eqs. (A13) and (A14) do not yield the same answer for $q \rightarrow 0$, indicating that the thermodynamic

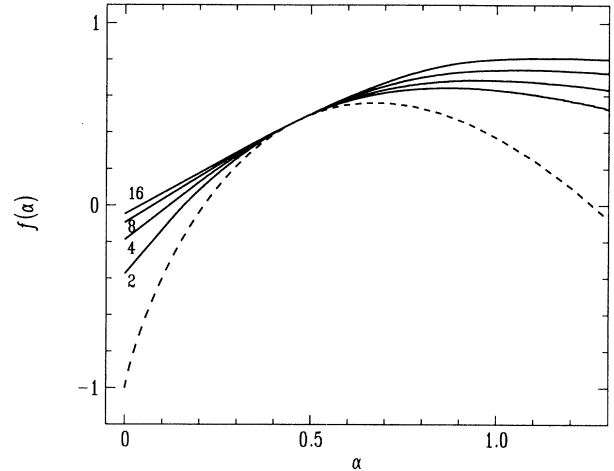


FIG. 13. Scaling functions $f_n(\alpha)$ of a binary random multiplicative process with refinement of lengths. Solid lines, completely correlated refinement steps, number of steps $n = 2, 4, 8, 16$, respectively. This scaling function has the same asymptotic ($n = \infty$) limit as the one in Fig. 3, dashed line, independent refinements.

limit $n \rightarrow 0$ does not exist in this case. The intricacies of this situation are discussed in [8].

The spectrum of scalings $f(\alpha)$, both for uncorrelated refinements and for completely correlated refinements at various values of n , is shown in Fig. 13. The spectra bear a striking similarity to those of Fig. 3, which were computed for the case of a binary cascade with measure refinements. We conclude that the general behavior of the dimension spectra is apparently determined by the level to level correlation rather than by details of the refinement process.

APPENDIX B: RANDOM MEASURE WITH COMPLETE CORRELATION

Here we sketch the evaluation of the integral $I_n(q)$ in Eq. (23) for large n . Note that the obvious restriction $q > 0$ applies. The behavior of the integral for large n follows from expanding the integrand around $x = \frac{1}{2}$. Let $x = \frac{1}{2}(1+t)$; then

$$I_n(q) = \left(\frac{1}{2}\right)^{qn-1} \int_0^1 h^n(t) dt, \quad (\text{B1})$$

with $h(t) = (1+t)^q + (1-t)^q$.

We have to discern the cases $q < 1$ and $q > 1$. For $q < 1$ the function h has an (absolute) quadratic maximum $h = 2$ at $t = 0$. Because h is raised to a large power, only a very small neighborhood of $t = 0$ contributes to the integral. Therefore, $(h/2)^n \approx [1 + q(q-1)t^2]^n$ and

$$I_n(q) \approx \left(\frac{1}{2}\right)^{nq-1} 2^n \int_0^{[q(1-q)]^{-1/2}} [1 + q(q-1)t^2]^n dt. \quad (\text{B2})$$

After the transformation $t' = t/n^{1/2}$ we recognize an approximation to an exponential function in the integrand and

$$I_n(q) \approx 2^{n(1-q)} \left[\frac{\pi}{nq(1-q)} \right]^{1/2}. \quad (\text{B3})$$

The resulting scaling function is

$$\tau_n(q) = q - 1 - \frac{1}{n \ln 2} C(q) + \frac{\ln n}{2n \ln 2}, \quad (\text{B4})$$

with $C(q) = \{\ln[\pi/q(1-q)]\}/2$.

For $q > 1$ the function h has a maximum $h = 2^q$ at $t = 1$. Because h is raised to a large power, only a very small neighborhood of $t = 1$ contributes to the integral. Therefore, $[h/(2q)]^n \approx [1 - q(1-t)/2]^n$ and

$$I_n(q) \approx \left(\frac{1}{2}\right)^{nq-1} 2^{qn} \int_{1-(2/q)}^1 [1 - q(1-t)/2]^n dt. \quad (\text{B5})$$

After the transformation $t' = 1 - t/n$ we recognize an approximation to an exponential function in the integrand and

$$I_n(q) \approx \frac{4}{nq}. \quad (\text{B6})$$

The resulting scaling function is

$$\tau_n(q) = -\frac{2}{n} + \frac{\ln q}{n \ln 2} + \frac{\ln n}{n \ln 2}. \quad (\text{B7})$$

APPENDIX C: CORRELATION STRUCTURE

The model of Sec. IID with piecewise constant conditional probabilities allows the analytical computation of correlation functions and the numerical computation of partition sums in terms of simple recursive formula's.

The correlation function $C(i, i')$ in Eq. (10) is most appropriately evaluated in terms of a generating function F_n defined by

$$F_n(q_1, \dots, q_n) = \int_0^1 dx_1 x_1^{q_1} \int_0^1 dx_2 x_2^{q_2} P(x_2 | x_1) \dots \times \int_0^1 dx_n x_n^{q_n} P(x_n | x_{n-1}). \quad (\text{C1})$$

From the symmetry between the x_i 's we have, for $i = 2, \dots, n$,

$$\langle x_i \rangle = \langle x_1 \rangle = F_1(1) = \frac{1}{2}. \quad (\text{C2})$$

Similar symmetry arguments yield

$$\langle x_i^2 \rangle = \langle x_1^2 \rangle = F_1(2) = \frac{1}{3}. \quad (\text{C3})$$

Because the fractal is built up in a strictly recursive manner, we have $C(i+j, i'+j) = C(i, i')$ for all positive integers j . Substitution of Eqs. (C2)–(C4) into Eq. (10)

yields

$$C(1, n) = 12F_n(1, 0, \dots, 0, 1) - 3. \quad (\text{C4})$$

It therefore remains to calculate the factor

$$\langle x_1 x_n \rangle = F_n(1, 0, \dots, 0, 1). \quad (\text{C5})$$

We recall that the conditional probabilities $P(x_i | x_{i-1})$ of the piecewise constant model are defined as

$$P(x_i | x_{i-1}) = \gamma + m(1 - \gamma)\delta_{i, i-1}, \quad (\text{C6})$$

where the Kronecker δ is unity if x_i and x_{i-1} are in the same interval and zero elsewhere. For clarity we will first derive the correlation function for the trivial case $\gamma = 0$. In this case x_1, \dots, x_n are all in the same interval. The integral over x_1 in Eq. (C1) therefore reduces to a summation over all m intervals of the grid

$$F_n(1, 0, \dots, 0, 1) = F_2(1, 1) = \frac{m}{4} \sum_{k=1}^m (\epsilon_k^2 - \epsilon_{k-1}^2)^2, \quad (\text{C7})$$

where $\epsilon_k = k/m$. Using the relation

$$\sum_{k=1}^m k^2 = \frac{1}{6} m(2m^2 + 3m + 1), \quad (\text{C8})$$

we obtain that

$$\langle x_1 x_n \rangle = F_2(1, 1) = \frac{1}{3} \left[1 - \frac{1}{(2m)^2} \right]. \quad (\text{C9})$$

Substituting Eq. (C2), (C3), and (C9) into the definition Eq. (10) of the correlation function, we obtain

$$C(1, n) = \begin{cases} 1, & n = 1 \\ 1 - \frac{1}{m^2}, & n \geq 2. \end{cases} \quad (\text{C10})$$

The correlation function $C(1, n)$ jumps from 1 to $1 - 1/m^2$ at $n = 1$ and the correlation length is infinite.

For the more interesting case $\gamma \neq 0$ it is easily seen that $\langle x_i \rangle$ and $\langle x_i^2 \rangle$ are again given by Eqs. (C2) and (C3). The average $\langle x_1 x_n \rangle$ follows from Eq. (C5), but the reduction Eq. (C7) no longer holds in this case. Careful evaluation of $F_n(1, 0, \dots, 0, 1)$ for increasing values of n reveals a recurrent structure. If we define a function

$$G_m = \frac{4}{3} \left[1 - \frac{1}{(2m)^2} \right], \quad (\text{C11})$$

the F_n can be expressed in terms of G_m ,

$$F_2(1, 1) = \frac{1}{4} [\gamma + (1 - \gamma)G_m], \quad (\text{C12})$$

$$F_3(1, 0, 1) = \frac{1}{4} \{ \gamma + (1 - \gamma)[\gamma + (1 - \gamma)G_m] \},$$

and, in general, F_{n+1} is obtained from F_n by replacement of the factor G_m by the factor $\gamma + (1 - \gamma)G_m$. Substitution of the F_n obtained this way into the right-hand side of (C4) yields the correlation function for $n > 1$

$$C(1, n) = (1 - \gamma)^{n-1} \left(1 - \frac{1}{m^2} \right). \quad (\text{C13})$$

This can be written in the more convenient form

$$C(1, n) = \begin{cases} 1, & n = 1 \\ \left(1 - \frac{1}{m^2}\right) \exp\left(-\frac{n-1}{\xi}\right), & n > 1 \end{cases} \quad (\text{C14})$$

with the correlation depth ξ defined as

$$\xi = -\frac{1}{\ln(1-\gamma)}. \quad (\text{C15})$$

APPENDIX D: RECURRENCE RELATION FOR THE PARTITION SUM

There are no analytical expressions for $\tau(q)$ available for the cascade model with intermediate correlations in Sec. IID. However, the piecewise constant form of the conditional probability distribution function allows for a very efficient numerical procedure. We will derive a simple recursive form for the computation of the partition sum. The procedure is shown first for the $j = 1$ term in Eq. (9),

$$\begin{aligned} \langle p_{n,1}^q \rangle &= \int_0^1 dx_1 x_1^q P(x_1) \int_0^1 dx_2 x_2^q P(x_2 | x_1) \cdots \\ &\times \int_0^1 dx_n x_n^q P(x_n | x_{n-1}). \end{aligned} \quad (\text{D1})$$

Other terms in Eq. (9) will have one or more x_i^q replaced by $(1-x_i)^q$. Because the first x_1 is (unconditionally) drawn from a uniform distribution, we write the integrations as

$$\langle p_{n,1}^q \rangle = \int_0^1 dx_1 x_1^q F_{n-1}(x_1, q). \quad (\text{D2})$$

The function $F_{n-1}(x_1, q)$ does not depend on the value of x_1 itself, but only on the interval containing x_1 , say, $[\epsilon_k, \epsilon_{k-1}]$ with $\epsilon_k = k/m$. We may therefore write $F_{n-1}(x_1, q) = F_{n-1}(k, q)$. The integral in Eq. (D2) then reduces to a summation

$$\langle p_{n,1}^q \rangle = \frac{1}{m(q+1)} \sum_{k=1}^m t_k(q) F_{n-1}(k, q) \quad (\text{D3})$$

with $t_k(q) = \epsilon_k^{q+1} - \epsilon_{k-1}^{q+1}$.

It turns out that $F_{n-1}(k, q)$ is a polynomial in $t_k(q)$ of degree $n-1$,

$$F_{n-1}(k, q) = \frac{1}{(q+1)^{n-1}} \sum_{i=0}^{n-1} c_i^{(n-1)} t_k^i(q). \quad (\text{D4})$$

The coefficients $c_k^{(n)}$ can be calculated recursively. For that purpose it is convenient to introduce the notation

$$\begin{aligned} \tilde{\gamma} &= m(1-\gamma), \\ S_n(q) &= \sum_{k=1}^m t_k^{n+1}(q). \end{aligned} \quad (\text{D5})$$

The number $\tilde{\gamma}$ is just the height of the spike in Fig. 4 above the background probability γ . From this definition we also see that $S_0(q) = S_0 = 1$. For later convenience we shall consequently write down this term. Substitution of Eq. (D4) into Eq. (D3) yields

$$\langle p_{n,1}^q \rangle = F_n(q) = \frac{1}{(q+1)^n} \sum_{i=0}^{n-1} c_i^{(n-1)} S_i(q). \quad (\text{D6})$$

The coefficients $c_i^{(n)}$ at level n can be expressed in terms of those at level $n-1$. To illustrate this we evaluate $F_n(k, q)$ for $n = 1, 2$, and 3

$$\begin{aligned} F_1(k, q) &= \frac{1}{(q+1)} [\gamma S_0 + \tilde{\gamma} t_k(q)] \\ &= \frac{1}{(q+1)} [c_0^{(1)} + c_1^{(1)} t_k(q)], \\ F_2(k, q) &= \frac{1}{(q+1)^2} \{ \gamma [\gamma S_0^2 + \tilde{\gamma} S_1(q)] \} + \frac{1}{(q+1)} \tilde{\gamma} t_k(q) F_1(k, q) \\ &= \frac{1}{(q+1)^2} \{ \gamma [c_0^{(1)} S_0 + c_1^{(1)} S_1(q)] + \tilde{\gamma} c_0^{(1)} t_k(q) + \tilde{\gamma} c_1^{(1)} t_k^2(q) \} \\ &= \frac{1}{(q+1)^2} [c_0^{(2)} + c_1^{(2)} t_k(q) + c_2^{(2)} t_k^2(q)], \\ F_3(k, q) &= \frac{1}{(q+1)^3} \{ \gamma [c_0^{(2)} S_0 + c_1^{(2)} S_1(q) + c_2^{(2)} S_2(q)] \} + \frac{1}{(q+1)^2} \tilde{\gamma} t_k(q) F_2(k, q) \\ &= \frac{1}{(q+1)^3} [c_0^{(3)} + c_1^{(3)} t_k(q) + c_2^{(3)} t_k^2(q) + c_3^{(3)} t_k^3(q)]. \end{aligned} \quad (\text{D7})$$

We observe the following substitution rules. For $n = 1$ we have

$$c_0^{(1)} = \gamma S_0, \quad c_1^{(1)} = \tilde{\gamma} \quad (\text{D8})$$

and for $n > 1$

$$c_0^{(n)} = \gamma \sum_{i=0}^{n-1} c_i^{(n-1)} S_i(q), \quad (\text{D9})$$

$$c_i^{(n)} = \tilde{\gamma} c_{i-1}^{(n-1)}, \quad i = 1, \dots, n-1.$$

The remaining task is now to compute the other terms in the partition sum that have one or more x_i^q replaced by $(1-x_i)^q$. It is a simple observation that these terms are automatically included by replacing $t_k(q)$ in the above expressions by

$$\tilde{t}_k(q) = t_k(q) + t_{m+1-k}(q). \quad (\text{D10})$$

The sum $S_n(q)$ is now taken over $\tilde{t}_k(q)$ with the obvious consequence that now $S_0 = 2$.

-
- [1] G. Parisi and U. Frisch, in *Turbulence and Predictability in Geophysical Fluid Dynamics and Climate Dynamics*, Proceedings of the International School of Physics "Enrico Fermi," Course LXXXVIII, Varenna, 1983, edited by M. Ghil, R. Benzi, and G. Parisi (North-Holland, Amsterdam, 1985), p. 84.
- [2] F. Anselmetti, Y. Gagne, E.J. Hopfinger, and R.A. Antonia, *J. Fluid Mech.* **140**, 63 (1984).
- [3] A.B. Chhabra and K.R. Sreenivasan, *Phys. Rev. Lett.* **68**, 2762 (1992).
- [4] A.B. Chhabra, C. Meneveau, R.V. Jensen, and K.R. Sreenivasan, *Phys. Rev. A* **40**, 5284 (1989).
- [5] A.B. Chhabra and K.R. Sreenivasan, *Phys. Rev. A* **43**, 1114 (1991).
- [6] C.W. Van Atta and T.T. Yeh, *J. Fluid Mech.* **59**, 537 (1973); **71**, 417 (1975).
- [7] E.A. Novikov, *Phys. Fluids A* **2**, 814 (1990).
- [8] M.H. Jensen, G. Paladin, and A. Vulpiani, *Phys. Rev. E* **50**, 4352 (1994).
- [9] B.B. Mandelbrot, *Physica A* **163**, 306 (1990).
- [10] C.J.G. Evertsz and B.B. Mandelbrot, *Physica A* **185**, 77 (1992).
- [11] A critical evaluation of the so-called Taylor hypothesis can be found in R.A. Antonia, N. Phan-Tien, and J.A. Chambers, *J. Fluid Mech.* **100**, 193 (1980).
- [12] A.S. Monin and A.M. Yaglom, *Statistical Fluid Mechanics* (MIT Press, Cambridge, MA, 1975).
- [13] K.R. Sreenivasan, *J. Stat. Phys.* (to be published).
- [14] G. Huber and P. Alström, *J. Phys. A* **24**, L1105 (1991), consider models with a variable base whose multipliers are normalized by fitting them in hyperspheres with increasing dimension.